

Kinetic theory of quantum transport at the nanoscale

Ralph Gebauer

*The Abdus Salam International Centre for Theoretical Physics (ICTP), 34014 Trieste, Italy
INFN Democritos National Simulation Center, 34013 Trieste, Italy*

Roberto Car

*Department of Chemistry and Princeton Institute for the Science and Technology of Materials,
Princeton University, Princeton, New Jersey 08540*

(Dated: November 1, 2018)

We present a quantum-kinetic scheme for the calculation of non-equilibrium transport properties in nanoscale systems. The approach is based on a Liouville-master equation for a reduced density operator and represents a generalization of the well-known Boltzmann kinetic equation. The system, subject to an external electromotive force, is described using periodic boundary conditions. We demonstrate the feasibility of the approach by applying it to a double-barrier resonant tunneling structure.

PACS numbers: 71.15.Pd, 72.10.-d, 72.10.Bg

I. INTRODUCTION

There is currently large interest in the development of electronic devices that operate at the molecular level, since these may revolutionize the electronic industry¹. Modeling electron transport at the nanoscale poses great theoretical challenges because in this regime the semi-classical Boltzmann kinetic equation commonly used to describe transport is not applicable. Boltzmann's equation treats the electrons in terms of their classical probability distribution in phase space, and deals with collision events quantum-mechanically using Fermi's golden rule². This formalism explains why conduction electrons subject to a uniform electric field do not accelerate indefinitely, but settle in a steady state regime of constant current, as a consequence of inelastic collisions with the lattice that lead to energy dissipation.

To describe transport in devices having spatial dimensions of the order of the electron wavelength, Boltzmann's equation should be replaced by a quantum mechanical Liouville-master equation for a reduced density operator^{2,3,4,5,6}. Such quantum kinetic approaches to electron transport have to deal with several difficulties. Probably most severe are those related to the description of boundary conditions between the device active region and the contacts: In most common approaches electrons can be exchanged between the device and its environment through left (L) and right (R) contacts with the electrodes of a battery. The $L(R)$ injected electrons are assumed to have thermal equilibrium distributions defined by the temperature T and the electrochemical potentials $\mu_{L(R)}$ of the electrodes. In self-consistent calculations, however, modifications of the distribution of the injected carriers, like drifting the momentum of the distribution or displacing the chemical potentials of the contacts, are necessary to avoid unphysical charging of the contacts⁷. Overall the issue of contacts and boundary conditions is crucial in all models of quantum transport^{6,7,8,9,10,11,12}.

In this paper we present a kinetic formulation which

avoids these difficulties by adopting periodic boundary conditions. The active region together with a part of the contacts is placed in a unit cell that is repeated periodically. One can imagine such a geometry as an infinite ring, without open boundaries. In this way we deal with a closed circuit with no exchanges of electrons with the environment^{13,14,15}. A current is induced in the circuit by an externally applied electromotive force.

In our approach coupling between the electrons and the lattice is included explicitly to prevent the electrons from accelerating indefinitely. This coupling is treated in perturbation theory (weak coupling). Furthermore, the time scale of inelastic electron-phonon collisions is typically much faster than the current relaxation time and is eliminated by a *coarse graining* procedure. The resulting Markovian dynamics of the reduced electron density operator is described by a Liouville-master equation, which effectively generalizes Boltzmann's equation at the nanoscale^{4,5}. We treat the diagonal and off-diagonal elements of the density operator on equal footing.

One common problem of kinetic master equations that describe collisions using Fermi's golden rule is that current continuity is violated in inhomogeneous media when the current density is defined in the standard way^{4,9}. In our approach, continuity is exactly satisfied, by properly taking into account the current contribution due to electron-phonon collisions, as described elsewhere¹⁶.

The reminder of this paper is organized as follows. In section II we describe the methods that we use. In particular, we recall how a Liouville master equation for an electron in contact with an external heat bath is derived (section II A). We then discuss electric fields (section II B), the definition of currents (section II C), and a generalization of the formalism to many particle systems (II D). Finally, in section III, we demonstrate the scheme with a numerical application to a system consisting of a one-dimensional wire connected to a double-barrier resonant tunneling structure (DBRTS). This example illustrates the key features of our approach and

the differences between our treatment and open boundary formulations^{7,9,10,17}.

II. METHOD

A. Liouville master equation

For simplicity we use in the following a one-dimensional notation, but extension to three-dimensions is straightforward. A ring of length L is a simple periodic structure. Ideally we should consider an infinite ring ($L \rightarrow \infty$). In numerical applications, however, L must be finite. This could be achieved by placing many periodically repeated unit cells of length L in a ring, but in the following we shall consider only the case of a single periodic unit having length equal to the perimeter of the ring. In absence of the external electric field the single-electron Hamiltonian is $H_0 = 1/2p^2 + U(x) = \sum_n \varepsilon_n c_n^\dagger c_n$, where $U(x)$ is a potential with periodicity L , the sum is over eigenstates of energy ε_n , and c_n^\dagger (c_n) are electron creation (annihilation) operators. Atomic units ($e = \hbar = m = 1$) are adopted throughout. The harmonic phonon bath has Hamiltonian $R = \sum_\alpha \omega_\alpha a_\alpha^\dagger a_\alpha$, where the sum is over eigenmodes of frequency ω_α , and a_α^\dagger (a_α) are phonon creation (annihilation) operators. The electron-phonon coupling potential is $V = \sum_{m,n,\alpha} \gamma_{m,n}^\alpha c_m^\dagger c_n a_\alpha^\dagger + h.c.$, in terms of matrix elements $\gamma_{m,n}^\alpha$ ($h.c.$ denotes the hermitian conjugate). The Hamiltonian of the total system (electron + bath) is $H_T = H_0 + R + V$. The density operator for the total system Σ satisfies the Liouville equation $\frac{d\Sigma}{dt} = -i[H_T, \Sigma]$. The reduced density operator for the electronic subsystem, S , is obtained from Σ by tracing out the bath degrees of freedom, *i.e.* $S = \text{Tr}_R \Sigma$. The equation of motion for S can be derived using a standard procedure^{18,19} in which V is treated to second order in perturbation theory, and a Markov approximation is made, whereby electron-phonon collisions become instantaneous processes described by Fermi's golden rule. The bath is assumed to be in thermal equilibrium at all times, *i.e.* any retroaction of the electron system on the bath is neglected. Then the Liouville-master equation for S is^{18,19}:

$$\frac{dS}{dt} = -i[H_0, S] + \mathcal{L}[S], \quad (1)$$

Here the term that describes collisions with the bath is

$$\mathcal{L}[S] \equiv - \sum_{m,n} \Gamma_{mn} (L_{nm} L_{mn} S + SL_{nm} L_{mn} - 2L_{mn} S L_{nm}), \quad (2)$$

where $L_{nm} = c_n^\dagger c_m$, and the transition probabilities Γ_{mn} are given by:

$$\Gamma_{mn} = \begin{cases} \mathcal{D}(\varepsilon_n - \varepsilon_m) |\gamma_{mn}|^2 (\bar{n}_{\varepsilon_n - \varepsilon_m} + 1) & \varepsilon_n > \varepsilon_m \\ \mathcal{D}(\varepsilon_m - \varepsilon_n) |\gamma_{mn}|^2 \bar{n}_{\varepsilon_m - \varepsilon_n} & \varepsilon_m > \varepsilon_n. \end{cases} \quad (3)$$

Here \bar{n}_ω is the thermal occupation and $\mathcal{D}(\omega)$ is the density of states of phonons with frequency ω . Eq. (3) ensures detailed balance leading the electron subsystem to thermal equilibrium in absence of an applied external electric field.

In our scheme, we calculate the time evolution of the density matrix, including diagonal and off-diagonal elements. In approaches using open boundary conditions, it is common practice to limit the description to the diagonal elements of the density matrix only⁴. It should be stressed, however, that the representation of the density matrix is very different when open boundary conditions are used instead of periodic boundary conditions. In open boundary approaches the different chemical potentials of the L and R contacts cause a breaking of symmetry between the contacts, and the final state is largely determined by the different occupations of the L and R incident channels. These occupations are given by the diagonal elements of the density matrix in the open boundary representation. In our approach, where periodic boundary conditions are adopted, we need to use *unperturbed eigenfunctions* as basis states. These states do not carry current, and the final, current-carrying state of the system is dominated by the off-diagonal elements of the density matrix in this basis. The computational complexity remains limited, however, because not all the elements of the density matrix need to be considered, but only those that fall within a finite energy window around the Fermi energy.

B. External static electric field

We include an external uniform static electric field \mathcal{E} by letting $p \rightarrow p - 1/cA(t)$. The Hamiltonian becomes $H(t) = 1/2(p - 1/cA(t))^2 + U(x)$. The vector potential is $A(t) = -c\mathcal{E}t$. This choice of the gauge (*v-gauge*) is compatible with periodic boundary conditions. We avoid the difficulty with a Hamiltonian that grows indefinitely with time by systematically performing gauge transformations in which the electronic wavefunctions are multiplied by a phase factor $\exp(-iA(t)/c \cdot x)$ and $A(t)$ in the Hamiltonian is restored to its initial value $A(t=0)$ ²⁰. In this way all the time dependence is transferred to S and the Hamiltonian remains constant. In order not to violate periodic boundary conditions the gauge transformations are only possible at times that are integer multiple of $\tau_\mathcal{E} = \frac{2\pi}{L\mathcal{E}}$. The time $\tau_\mathcal{E}$ is arbitrarily small for $L \rightarrow \infty$, but is always finite in numerical applications. In practice we proceed as follows. Let $A(0) = 0$ at $t = 0$. First we integrate Eq. (1) for the time period $\tau_\mathcal{E}$ using the Hamiltonian propagator with the electric field, which corresponds to the first term in the right hand side (r.h.s.) of Eq. (1). Then we apply a gauge transformation to set the vector potential to zero. Finally, we propagate S for the same period $\tau_\mathcal{E}$ using the collision propagator, which corresponds to the second term on the r.h.s. of Eq.(1). The result is a density matrix $S(\tau_\mathcal{E})$. This procedure is

repeated at all subsequent time steps in increments of $\tau_{\mathcal{E}}$. In the limit of $\tau_{\mathcal{E}} \rightarrow 0$ this procedure converges to the exact kinetic propagation.

Our approach in which a static external electric field acts as driving force for the electrons, is well suited to dealing with systems where the voltage drop occurs along one given direction in space. Complex geometries in devices with many-terminals⁸ may not be tractable in this framework. However, many current applications of nano-scale transport, like *e.g.* break junctions, STM tips, or interlayer tunneling, can be represented within our scheme.

C. Hamiltonian and dissipative currents

The current density associated to Hamiltonian propagation is

$$\begin{aligned} j(x;t) &= \text{Tr} \left[S(t) \hat{J}(x;t) \right], \\ \hat{J}(x;t) &= \frac{1}{2} \left[(\hat{p} - 1/cA(t)) \delta(x - \hat{x}) \right. \\ &\quad \left. + \delta(x - \hat{x}) (\hat{p} - 1/cA(t)) \right], \end{aligned} \quad (4)$$

where the current (as well as all other observables) is averaged over the period $\tau_{\mathcal{E}}$. It is important to note that these definitions do not yield a current that satisfies the continuity equation

$$\left\langle x \left| \frac{dS(t)}{dt} \right| x \right\rangle + \frac{d}{dx} j(x;t) = 0. \quad (5)$$

In contrast, Eq. (5) is satisfied by the *physical current* $j_T(x;t) = j(x;t) + j_{\mathcal{L}}(x;t)$, which includes a contribution $j_{\mathcal{L}}$ due to the coupling with the phonon bath. An explicit expression for $j_{\mathcal{L}}(x;t)$ is given in Ref. 16. In all numerical applications below we report the total physical current $j_T(x;t)$.

D. Many particle formulation

In the many electron case, Eq. (1) is still valid, but should be reduced to an effective single-particle form in practical applications. This is straightforward if we adopt the time dependent Hartree approximation. In this approximation the many-particle system is mapped onto a system of non-interacting particles, subject to a time-dependent Hartree potential defined in terms of the instantaneous electronic charge density²². The Hartree interaction is crucial to modeling charge rearrangement effects when the system is driven away from equilibrium.

The single-particle Hamiltonian in presence of an electric field is $H(t) = 1/2 (p - 1/cA(t))^2 + U(x) + \Delta\Phi(x;t)$, where $\Delta\Phi$ is the periodic Hartree potential given by $\Delta\Phi(x;t) = \int dx' \frac{\Delta n(x';t)}{|x-x'|}$, where Δn is the charge density perturbation induced by the field.

The independent particle system is described by a single particle density operator S^1 , given by $S^1 = \sum_{lm} f_{lm} |l\rangle\langle m|$ in the basis of the eigenstates of H_0 , *i.e.* the equilibrium single particle eigenstates. The expansion coefficients f_{lm} are related to the many particle operator S via $f_{lm} = \text{Tr} [S c_m^\dagger c_l]$. This procedure is discussed *e.g.* in Ref. 21. The equation of motion for f_{lm} then follows from Eq. (1). Using $\text{Tr} [S c_n^\dagger c_m^\dagger c_p c_q] = f_{qn} f_{pm}$ (neglecting the exchange term $-f_{qm} f_{pn}$), one finds:

$$\begin{aligned} \frac{df_{nm}}{dt} &= -i \sum_p (H_{np}(t) f_{pm} - f_{np} H_{pm}(t)) \\ &\quad + (\delta_{nm} - f_{nm}) \sum_p (\Gamma_{np} + \Gamma_{mp}) f_{pp} \\ &\quad - f_{nm} \sum_p (\Gamma_{pn} + \Gamma_{pm}) (1 - f_{pp}). \end{aligned} \quad (6)$$

Here $H_{nm}(t)$ are Hamiltonian matrix elements between the equilibrium single-particle eigenstates. In Eq. (6) the diagonal elements f_{nn} satisfy $0 \leq f_{nn} \leq 1$ in accordance with Pauli's principle, and the total number of electrons is conserved. At equilibrium and in absence of an electric field, Eq. (6) gives $f_{nm} = \delta_{nm} / (1 + \exp(\beta(e_n - \mu)))$, *i.e.* a Fermi-Dirac distribution in which the chemical potential μ is determined by the condition $\sum_n f_{nn} = N$, where N is the total number of electrons. In presence of a static electric field Eq. (6) leads to a stationary distribution in which the effect of the field is balanced by the effect of inelastic phonon scattering. In the following we find the stationary distribution by setting $\dot{f} = 0$ in Eq. (6) and solve the resulting equation by a self-consistent procedure.

III. APPLICATION TO A DBRTS

To illustrate how this works in practice we consider a DBRTS as a test system. The potential $U(x)$ in absence of an applied electric field is shown in the upper panel of Fig. 1. Outside the barrier region, we assume a carrier density of $4.3 \cdot 10^{18} \text{cm}^{-3}$, and choose an effective mass of $0.1m_e$ and a dielectric constant of 10. Due to the large dimensions of the DBRTS in the directions perpendicular to the barriers, an effective one-dimensional model can be assumed. We adopt a model in which the phonon density of states $\mathcal{D}(\omega) \propto \omega^2$, and the electron-phonon couplings $\gamma_{nm} = \gamma_0$ for all states n, m . We choose values of 0.136meV and of 0.218meV , respectively, for γ_0 , and a temperature of $T = 25.3 \text{K}$, such that $k_B T$ is comparable to the electronic level spacing at the Fermi energy in our finite system ($L = 244 \text{nm}$). We solve Eq. (6) for steady state behavior, *i.e.* $\frac{df_{nm}}{dt} = 0$, and determine the Hartree potential $\Delta\Phi(x)$ self-consistently, for different values of the applied external field \mathcal{E} . The total potential acting on the electrons when \mathcal{E} corresponds to peak current is shown in the middle panel of Fig. 1. The total potential includes $U(x)$, the externally applied bias (represented

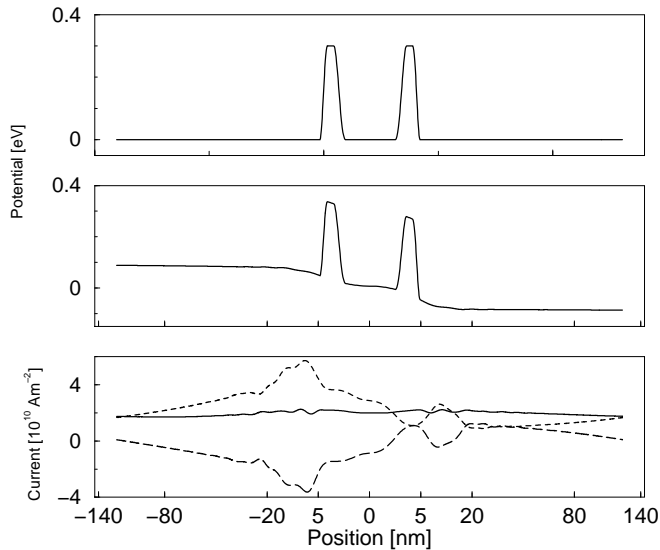


FIG. 1: Upper panel: the DBRTS in the absence of an electric field. Middle panel: total potential in the presence of external electric field for low γ_0 (see text). Lower panel: spatial distribution of the current. Short dashed line: Hamiltonian current $j(x)$. Long dashed line: Current due to inelastic collisions $j_{\mathcal{L}}(x)$. Solid line: Total current $j_T(x) = j(x) + j_{\mathcal{L}}(x)$. Within the numerical precision of the calculation j_T is constant as required by continuity (5). All plots use a non-linear scale for the position to magnify the barrier region.

by a linearly varying potential $\phi_{\mathcal{E}}(x) = -\mathcal{E} \cdot x$, and the Hartree potential. Notice that we adopt here, for visualization purposes, the position gauge (x -gauge) which is obviously incompatible with periodic boundary conditions. As we can see in the figure, the total potential has the same qualitative behavior found in self-consistent calculations using open boundary conditions for similar model systems. In our approach, however, the voltage drop across the barrier is an output rather than an input of the calculation. Another distinctive feature is that we observe not only a potential drop at the tunneling structure but also a small voltage drop along the wire. The latter is very small (about 5 % of the total in the case shown in Fig. 1), indicating that the external field is nearly completely screened inside the wire, as one should expect. In the lower panel of Fig. 1 we report the current densities $j(x)$, $j_{\mathcal{L}}(x)$, and $j_T(x)$ corresponding to the electric field and electron-phonon coupling of the middle panel. We calculate the current $j_{\mathcal{L}}$ by extending the single-particle theory of Ref. 16 to the many-electron case within the time dependent Hartree approximation. On the time scale of kinetic evolution the current j originates from Hamiltonian propagation, while the current $j_{\mathcal{L}}$ accounts for the charge flow due to inelastic phonon scattering and is larger at the contacts where deviations from equilibrium are larger. The effect is stronger at the injection contact where charge accumulates. The behavior of $j_{\mathcal{L}}$ indicates where local heating should be expected to occur.

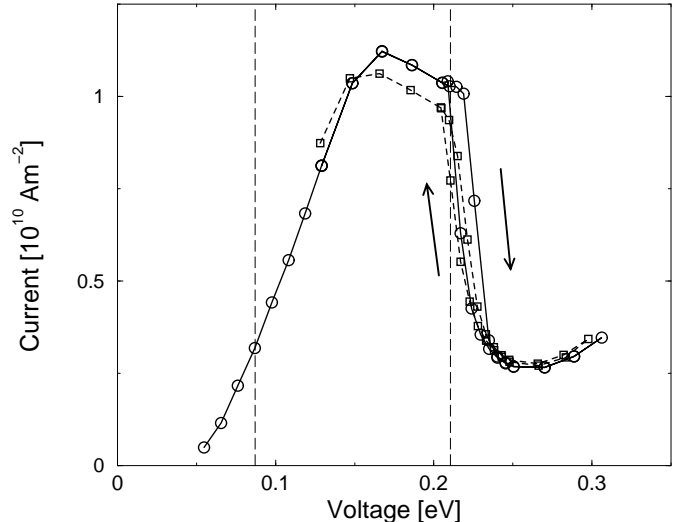


FIG. 2: Two calculated IV characteristics of a DBRTS. The curve with the highest peak current (solid line, circles) is the one corresponding to the lower value of γ_0 . The energy of the dashed line on the left corresponds to twice the energy difference between the resonant level and the Fermi level. The second dashed vertical line is displaced to the right by twice the energy band width. According to a simple model of resonance, transmission should occur in the region between the two lines.

Two $I-V$ characteristics, corresponding to two different values of the electron-phonon coupling parameter γ_0 , are reported in Fig. 2. The voltage in the figure is the drop across the barrier structure, rather than the total voltage drop $\mathcal{E} \cdot L$ in the simulation cell. The calculations simulate an adiabatic sweep from low to high voltage biases and viceversa: at each small increment (decrement) of the applied electromotive force we compute a new current and voltage drop using the induced potential obtained in the previous step as input for the self-consistent calculation. Interestingly, the characteristics at lower γ_0 exhibits an hysteresis loop which is much less pronounced in the characteristics at larger γ_0 . A larger electron-phonon coupling also shifts the peak of the resonance to lower voltages and reduces the peak to valley ratio. The hysteresis loop, which is suppressed by strong electron-phonon coupling, originates from charging of the resonant level, as already found in earlier calculations^{23,24}.

Even though it is not our aim here to reproduce a specific experiment, it is interesting to note that by appropriate choice of the parameters and conditions of the calculation, we can reproduce important experimentally observed features of a DBRTS like bistability and hysteresis effects²⁵.

In our approach inelastic collisions provide a source of non-linearity other than the tunneling structure. To better appreciate this effect we report in Fig. 3 the energy distribution of f_{nm} , *i.e.* the diagonal elements of the density matrix, for two values of V , a low voltage below peak current and a high voltage close to peak current,

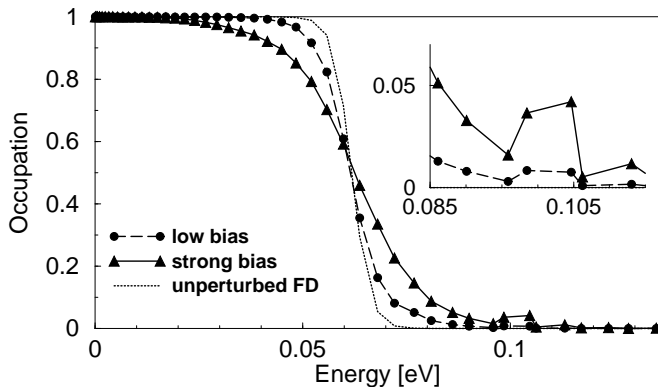


FIG. 3: The diagonal elements f_{nn} of the density matrix in the steady state. Stronger bias leads to a stronger deviation from the unperturbed Fermi-Dirac (FD) distribution.

respectively. We see that at low voltage the population is close to the thermal distribution at temperature T , whereas at high voltage the population resembles a thermal distribution at a temperature higher than T . This is a real physical effect: at larger biases the electron distribution deviates more from equilibrium. We also notice (see the inset of Fig. 3) that the most significant deviation from thermal equilibrium is a small peak in the tail of the distribution, in correspondence with the energy of the resonant state. This indicates charging of the resonant level, an effect which is at the origin of the intrinsic bistability of a DBRTS²⁶.

The effect of inelastic collisions on transport properties can be neglected in the weak bias limit (linear response regime)¹³. In this regime transport in mesoscopic and nanoscopic systems is governed by Landauer's formulas for the conductance²⁷, which can be derived within the Kubo formalism²⁸. This is usually done by adopting open boundary conditions, but recently a derivation

based on a ring geometry (in the limit $L \rightarrow \infty$) has also been reported²⁹. In the linear response regime the conductance can be calculated by applying a sinusoidal field and taking the limit $\omega \rightarrow 0$, in absence of coupling to the lattice. In our kinetic approach we look instead for the steady state solution under a constant applied field. This requires coupling to the lattice whenever \mathcal{E} is finite, and allows us to consider also strongly nonlinear regimes like in the DBRTS case discussed above.

IV. CONCLUSION

We have presented a kinetic approach to study quantum transport at the nanoscale, including the effect of inelastic collisions. The main physical approximations are a perturbation treatment of electron-phonon scattering and a Markov approximation in the dynamics. Use of simplified Hamiltonians, as in the example discussed above, is by no means necessary. A realistic description of the electronic structure within Time Dependent Current-Density Functional Theory^{30,31,32} is possible, and work to achieve this goal is at an advanced stage of development. More accurate models for the phonons and the electron-phonon coupling would be considered in the future. Our approach is not limited to steady-state phenomena, but could be applied to time-dependent transient behavior as well.

Acknowledgments

This work was supported by DOE under grant DE-FG02-01ER45928 and by the National Science Foundation (MRSEC Program) through the Princeton Center for Complex Materials (DMR 0213706).

¹ J.R. Heath and M.A. Ratner, *Physics Today* **56**, 43 (2003).

² See, e.g., J. Rammer, *Quantum Transport Theory* (Perseus Books, Reading, Massachusetts, 1998) or M. Toda, R. Kubo, N. Hashitsume, *Statistical physics. II: Nonequilibrium statistical mechanics, 2nd Ed.* (Springer, Berlin, 1991).

³ M.V. Fischetti, *Phys. Rev. B* **59**, 4901 (1999).

⁴ M.V. Fischetti, *J. Appl. Phys.* **83** 270 (1998).

⁵ F. Rossi, A. Di Carlo, and P. Lugli, *Phys. Rev. Lett.* **80**, 3348 (1998).

⁶ R.P. Zaccaria and F. Rossi, *Phys. Rev. B* **67**, 113311 (2003).

⁷ W. Pötz, *J. Appl. Phys.* **66**, 2458 (1989).

⁸ S.E. Laux, A. Kumar, and M.V. Fischetti, *J. Appl. Phys.* **95**, 5545 (2004).

⁹ W.R. Frensley, *Rev. Mod. Phys.* **62**, 745 (1990).

¹⁰ M.A. Talebian and W. Pötz, *Appl. Phys. Lett.* **69**, 1148 (1996).

¹¹ A. Nakano, R.K. Kalia, and P. Vashishta, *Appl. Phys. Lett.*

64, 2569 (1994).

¹² C. Lent and D. Kirkner, *J. Appl. Phys.* **67**, 6353 (1990).

¹³ W. Kohn and J.M. Luttinger, *Phys. Rev.* **108**, 590 (1957).

¹⁴ R. Landauer and M. Büttiker, *Phys. Rev. Lett.* **54**, 2049 (1985).

¹⁵ M. Büttiker, Y. Imry, and R. Landauer, *Phys. Lett.* **96A**, 365 (1983).

¹⁶ R. Gebauer and R. Car, submitted.

¹⁷ M. Büttiker, *IBM J. Res. Div.* **32**, 63 (1988).

¹⁸ W.H. Louisell, *Quantum Statistical Properties of Radiation* (Wiley, New York, 1973).

¹⁹ C. Cohen-Tannoudji, J. Dupont-Roc, and G. Grynberg, *Atom-photon interactions: basic processes and applications*, Wiley, New York (1992).

²⁰ W. Kohn, *Phys. Rev.* **133**, A171 (1964).

²¹ R. Hübner and R. Graham, *Phys. Rev. B* **53**, 4870 (1996).

²² P.A.M. Dirac, *Proc. Camb. Philos. Soc.* **26**, 376 (1930), A.D. McLachlan, *Mol. Phys.* **8**, 39 (1964).

²³ K.L. Jensen and F.A. Buot, *Phys. Rev. Lett.* **66**, 1078

- (1991).
- ²⁴ H. Mizuta and C. Goodings, *J. Phys.: Cond. Mat.* **3** 3739 (1991).
- ²⁵ V.J. Goldman, D.C. Tsui, and J.E. Cunningham, *Phys. Rev. Lett.* **58**, 1256 (1987).
- ²⁶ R. Gebauer and R. Car, in preparation.
- ²⁷ R. Landauer, *IBM J. Res. Dev.* **1**, 223 (1957); *Phil. Mag.* **21**, 863 (1970).
- ²⁸ D.J. Thouless, *Phys. Rev. Lett* **47**, 972 (1981).
- ²⁹ A. Kamenev and W. Kohn, *Phys. Rev. B* **63**, 155304 (2001).
- ³⁰ E. Runge and E.K.U. Gross, *Phys. Rev. Lett.* **52**, 997 (1984).
- ³¹ G. Vignale and W. Kohn, *Phys. Rev. Lett.* **77**, 2037 (1996).
- ³² K. Burke, R. Car and R. Gebauer, in preparation.